

## Horizontally directed growth of carbon nanotubes utilizing self-generated electric field from plasma induced surface charging

J. B. K. Law, C. K. Koo, and J. T. L. Thong<sup>a)</sup>

Department of Electrical and Computer Engineering, National University of Singapore,  
4 Engineering Drive 3, Singapore 117576, Singapore

(Received 4 June 2007; accepted 22 November 2007; published online 12 December 2007)

Plasma induced surface charging during carbon nanotube (CNT) growth via radio frequency plasma-enhanced chemical vapor deposition is exploited to direct the growth in a horizontal direction on a device substrate without the need for external biasing arrangements. Using a silicon-on-insulator substrate, a pair of electrodes is fabricated in which one electrode is shorted to the handle layer and the other is left floating. A potential difference results from the plasma, and creates a lateral electric field between the electrodes that is used to direct the growth of CNTs. The approach allows for wafer-scale growth of laterally aligned CNTs. © 2007 American Institute of Physics. [DOI: 10.1063/1.2824478]

During the past one and a half decades, a wide range of carbon nanotube (CNT)-based electronic devices have been demonstrated.<sup>1,2</sup> Although there have been proposals for vertical CNT device structures,<sup>3</sup> planar device geometries are more in line with conventional integrated circuit (IC) designs. There is a need for rational assembly techniques which allow precise and controlled positioning and alignment of these one-dimensional nanostructures at desired locations for connections to be made in a manner compatible with conventional IC manufacturing. Furthermore, scalable methodologies, as opposed to single-device fabrication approaches, are needed if devices incorporating CNTs are to become a commercial reality.

Several approaches have been explored to laterally align CNTs such as lattice-directed or atomic-step directed epitaxial growth,<sup>4,5</sup> controlled directed deposition through chemical modification of the surfaces of nanotubes or substrates,<sup>6,7</sup> and directed assembly under external forces such as by flow and electric fields.<sup>8-10</sup> In particular, the approach using electric-field assisted assembly has been actively explored as a viable integration strategy for lateral alignment of CNTs.<sup>11</sup> The use of electric field can be applied postgrowth<sup>9,12,13</sup> or during growth.<sup>10,14,15</sup> A major limitation of extant approaches is the requirement for voltages to be externally applied through prefabricated contacts pads. The need for external biasing poses a significant challenge for large-scale assembly of nanotubes where a significant number of contact pads or interconnects to the target electrodes are needed.

In this work, we revisit the use of an electric field to align CNTs during growth. However, unlike conventional methods which require voltages to be applied through contact pads during growth, we avoid the use of external biasing. Our working hypothesis was to exploit the plasma-induced surface charging phenomenon during the growth to create a lateral electric field between adjacent electrodes through rational electrode design on a substrate. Patterned catalyst islands on the desired electrodes define the CNT growth location, while the self-generated electric field directs the lateral growth of CNTs.

To consider how such an electric field could be created during growth, we consider the phenomenon of plasma-

induced surface charging commonly encountered in radio frequency (rf) plasma processing.<sup>16-18</sup> When an electrically insulating (floating) surface comes into contact with rf plasma, the potential of the surface ( $V_f$ ) tracks the plasma potential ( $V_p$ ), as shown in Eq. (1), since the difference between the two is the sheath potential ( $V_{sh}$ ), given by Eq. (2), which is roughly constant.<sup>19</sup>

$$V_f = V_p - V_{sh}, \quad (1)$$

$$V_{sh} = \frac{kT_e}{2e} \ln\left(\frac{M}{2.3m}\right), \quad (2)$$

where  $V_f$  is the floating potential of the insulating surface,  $T_e$  is the electron temperature, and  $m$  and  $M$  are the masses of the electrons and ions in the plasma, respectively.

In reality, a spatial nonuniformity in  $V_p$  exists across the plasma chamber due to nonuniformity in the plasma. The causes of plasma nonuniformity have been attributed to factors as discussed in Refs. 16 and 17. Due to a nonuniform  $V_p$ , an electrode that is isolated from the substrate by an insulating layer (e.g., SiO<sub>2</sub>) develops a floating potential  $V_{fe}$  with respect to the plasma potential at the position of the electrode in the chamber; the substrate develops a different floating potential ( $V_{fsub}$ ) determined by  $V_p$  at the wafer edge. Figure 1(a) illustrates plasma induced surface charging on an isolated electrode sitting on an insulator on a conducting substrate; a particle-in-cell plasma physics simulation software (OOPIC PRO) is used to model the dc floating potentials on the substrate subjected to plasma processing. The simulated results illustrate a difference in surface potential ( $\sim -100$  V) between the substrate and the isolated electrode when subjected to particles bombardment in a rf plasma. As a result of the potential difference between  $V_{fe}$  and  $V_{fsub}$ , a vertical electric field ( $E$  field) results across the insulator layer in Fig. 1(a). An important step in our work involves redirecting the electric field to be horizontally/laterally displaced across two adjacent electrodes. This could be achieved by using a pair of adjacent electrodes, one of which is floating, while the other is electrically connected to the conductive substrate through a conducting plug. In this way, when subjected to rf plasma, the pair of electrodes would yield different potentials at the surface, which would then give rise to a lateral  $E$  field between the electrodes. Simulation using OOPIC PRO was

<sup>a)</sup>Electronic mail: elettl@nus.edu.sg

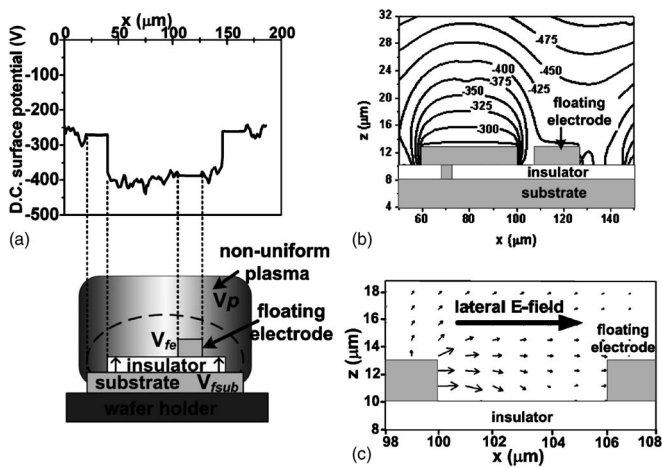


FIG. 1. OOPIC PRO simulation showing (a) difference in surface potential between the substrate and the isolated electrode in a plasma, (b) equipotential lines due to charging encountered by the geometry, and (c) electric field vectors in the vicinity of the gap between the electrode pair in (b).

conducted on this geometry. Figure 1(b) shows the simulated equipotential lines, while Fig. 1(c) shows the electric field vectors in the vicinity of the gap between the two electrodes. The electric field is predominantly in the horizontal direction pointing from the left electrode toward the right electrode.

We verified the presence of this potential difference by direct experimental measurement using a technique known as Stanford plasma on-wafer real time<sup>18</sup> to measure the potential difference of electrodes whose geometry is similar to that shown in Fig. 1(b) and under CNT growth conditions, but without catalyst. A potential difference from  $-110$  to  $-165$  V was measured at a rf power of between 20 and 40 W in the rf Plasma chamber, thereby verifying the presence of a potential difference between the isolated electrodes with respect to the substrate during rf plasma processing in our reactor system.

In order to demonstrate that this self-generated lateral electric field between adjacent electrodes during rf plasma could be utilized for directed CNT growth, the following device structure was fabricated. The typical process flow to fabricate the growth structure is shown in Fig. 2. (A detailed description can be found in the supplemental material EPAPS, S1.<sup>20</sup>) A silicon-on-insulator die consisting of a  $3\ \mu\text{m}$  thick highly doped ( $p^{++}$ ) silicon (Si) device layer on top of a  $2\ \mu\text{m}$  thick buried oxide (BOX) layer was used [Fig. 2(a)]. The die was lithographically patterned and dry etched to delineate pairs of  $p^{++}$  silicon electrodes isolated from the

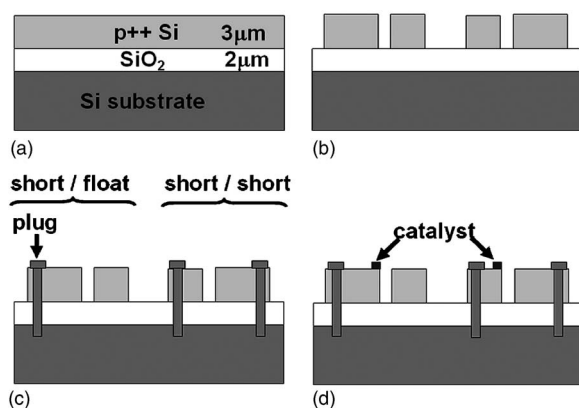


FIG. 2. Typical process flow to fabricate the test die.

Author complimentary copy. Redistribution subject to AIP license or copyright, see <http://apl.aip.org/apl/copyright.jsp>

substrate by the oxide layer [Fig. 2(b)]. To illustrate the validity of our hypothesis, two types of paired-electrode design were fabricated on the same die: (i) short/float and (ii) short/short. To short an electrode to the handle layer (substrate underlying the BOX), a platinum (Pt) plug was deposited in a focused-ion beam milled via hole [Fig. 2(c)]. The short/float configuration realizes the configuration illustrated in Figs. 1(b) and 1(c). The short/short configuration acts as a control, and is achieved by shorting both electrodes to the handle layer. With such a configuration, both electrodes will be at the same potential as the substrate during rf plasma processing and no lateral electric field is expected to exist between them. Figures 3(a) and 3(b) show scanning electron microscope (SEM) images of these two types of electrodes fabricated on the same die. The electrodes are spaced  $6\ \mu\text{m}$  apart, with a width of  $6\ \mu\text{m}$  and lengths of  $40\ \mu\text{m}/20\ \mu\text{m}$ . Iron (Fe) catalyst islands were next patterned on the top edge of one electrode from each pair using a second-level electron-beam lithography, followed by metallization and lift-off to predefine the locations for CNT growth [Fig. 2(d)].

rf plasma enhanced chemical vapor deposition (PECVD) (refer to supplemental material EPAPS, S2 for details of the system configuration<sup>20</sup>) was carried out in the same reactor chamber as described above, using  $\text{C}_2\text{H}_2$  and  $\text{NH}_3$  at a flow rate of 60 and 13 SCCM (SCCM denotes cubic centimeter per minute at STP), respectively, at 3.2 mbar process pressure. The substrate temperature was maintained at  $700\ ^\circ\text{C}$ , for a growth duration of 10 min. A rf power of 50 W was applied to generate the plasma, which produced a substrate direct current (dc) bias of  $\sim -30$  V.

The SEM image shown in Fig. 3(c) demonstrates the directed growth of CNTs from the short/float electrode pair. Lateral growth of multiwalled-CNTs (MWCNTs) was observed from the patterned catalyst toward the opposing electrode. In contrast, for the short/short electrode pair, the as-grown nanotubes did not exhibit any preferred alignment and grew randomly from the patterned catalyst [Fig. 3(d)]. It was noted that there was no apparent orientation of the MWCNTs in the vertical direction, although a vertical field should exist on the electrodes during plasma processing. This could be explained by the fact that a relatively low rf power (50 W) was used in our process, resulting in a small sheath potential and consequently small  $E$  field which was insufficient to cause vertical alignment. The rationale for choosing a low rf power is to ensure that the lateral electric field component is much greater than the vertical field component for the short/float electrode pair, such that the CNTs are directed to grow horizontally.

There is also a difference in the growth rate of the MWCNTs—the horizontally directed CNTs were not only longer, but the growth was noticeably denser, than those grown on the short/short electrode pairs. This is attributed to the lateral electric field which enhances the growth rate of the CNTs. Similar observations of enhanced growth rate of CNTs in the presence of high electric fields have been reported by others.<sup>21,22</sup>

Figure 3(e) shows a higher resolution SEM image of the horizontally aligned MWCNTs, revealing the morphology of the nanotubes. The MWCNTs grown are slightly curly, unlike straight CNTs grown by conventional PECVD where the vertical field is much larger due to a large rf/dc power applied. In fact, the morphology of the CNTs closely resembles that of vertically aligned CNTs grown by thermal CVD,<sup>23</sup>

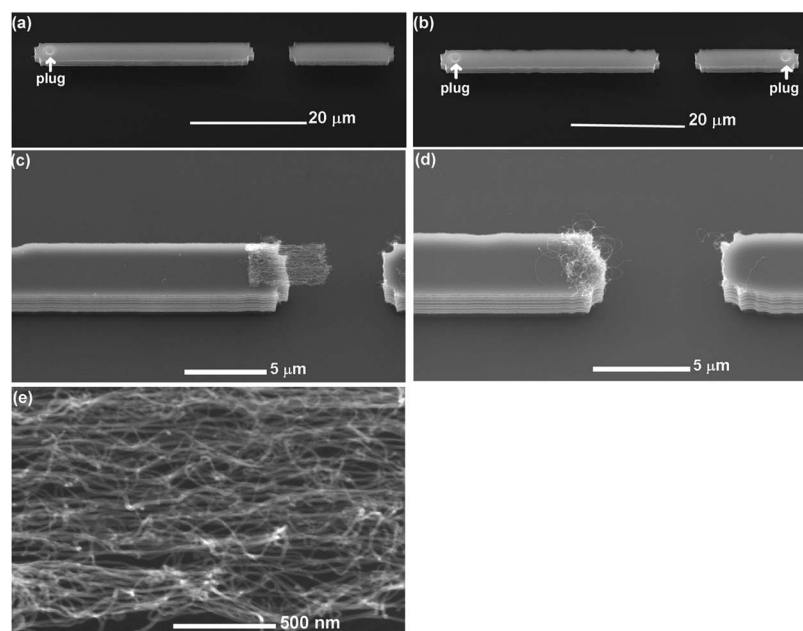


FIG. 3. SEM images showing (a) fabricated short/float electrode configuration, (b) fabricated short/short electrode configuration as control, (c) horizontally directed growth of MWCNTs from the short/float electrode pair, (d) randomly orientated growth of nanotubes from short/short configuration, and (e) higher resolution image of the aligned MWCNTs grown in (c).

though with lateral orientation. This suggests that the lateral field strength between the electrode pair was insufficient to affect the microstructure (high resolution transmission electron microscopy image of the MWCNT can be found in the supplemental material EPAPS, S3),<sup>20</sup> but yet was adequate to induce growth orientation. This has favorable implications, as normally, PECVD tends to make the CNTs grown defective because of the large rf/dc power needed to orientate the tubes.<sup>24,25</sup>

Our proposed technique offers an alternative method for *in situ* electric field directed growth of CNTs, with several advantages. The electric field required is self-generated during growth by the rf plasma. Therefore, there is no requirement for external biasing which requires microscale/millimeter-scale contact pads to apply the bias. In fact, the electrodes can be small isolated patterns separated by microscopic gaps that the CNTs are required to bridge. In addition, the technique is scalable and in principle this method can be used for directed growth of CNTs on a wafer scale.

In summary, we demonstrated a technique for laterally directed growth of CNT by utilizing the self-generated electric field created between electrodes during rf PECVD growth due to plasma charging. Simulation and direct experimental measurements were conducted to verify the presence of this self-generated electric field. The technique offers an alternative method using *E*-field directed growth of CNTs, with no requirement for external bias, or large-sized contact pads to apply bias. Being scalable, it could be used for whole-wafer directed growth of CNTs. The concept of creating lateral *E* field may potentially be applied to the directed growth of other materials using a rf plasma process.

This project is funded by a Grant No. 062 101 0023 from A\*STAR. The authors thank Dr. Akkipeddi Ramam, Eric Tang Xiaosong and Chen Yi Fan from IMRE for providing lithography and etching processing. J. B. K. Law acknowledges the NGS and A\*STAR for a Graduate Scholarship Award.

- <sup>1</sup>M. Terrones, *Annu. Rev. Mater. Res.* **33**, 419 (2003).
- <sup>2</sup>R. H. Baughman, A. A. Zakhidov, and W. A. de Heer, *Science* **297**, 787 (2002).
- <sup>3</sup>A. M. Cassell, J. Li, R. M. D. Stevens, J. E. Koehne, L. Delzeit, H. T. Ng, Q. Ye, J. Han, and M. Meyyappan, *Appl. Phys. Lett.* **85**, 2364 (2004).
- <sup>4</sup>H. Ago, K. Nakamura, K.-I. Ikeda, N. Uehara, N. Ishigami, and M. Tsuji, *Chem. Phys. Lett.* **408**, 433 (2005).
- <sup>5</sup>A. Ismach and E. Joselevich, *Nano Lett.* **6**, 1706 (2006).
- <sup>6</sup>M. Burghard, G. Duesberg, G. Philipp, J. Muster, and S. Roth, *Adv. Mater. (Weinheim, Ger.)* **10**, 584 (1998).
- <sup>7</sup>M. A. Meitl, Y. Zhou, A. Gaur, S. Jeon, M. L. Usrey, M. S. Strano, and J. A. Rogers, *Nano Lett.* **4**, 1643 (2004).
- <sup>8</sup>S. Huang, B. Maynor, X. Cai, and J. Liu, *Adv. Mater. (Weinheim, Ger.)* **15**, 1651 (2003).
- <sup>9</sup>X. Q. Chen, T. Saito, H. Yamada, and K. Matsushige, *Appl. Phys. Lett.* **78**, 3714 (2001).
- <sup>10</sup>Y. Zhang, A. Chang, J. Cao, Q. Wang, W. Kim, Y. Li, N. Morris, E. Yenilmez, J. Kong, and H. Dai, *Appl. Phys. Lett.* **79**, 3155 (2001).
- <sup>11</sup>L. X. Benedict, S. G. Louie, and M. L. Cohen, *Phys. Rev. B* **52**, 8541 (1995).
- <sup>12</sup>R. Krupke, F. Hennrich, H. B. Weber, M. M. Kappes, and H. v. Lohneysen, *Nano Lett.* **3**, 1019 (2003).
- <sup>13</sup>L. A. Nagahara, I. Amlani, J. Lewenstein, and R. K. Tsui, *Appl. Phys. Lett.* **80**, 3826 (2002).
- <sup>14</sup>A. Ural, Y. Li, and H. Dai, *Appl. Phys. Lett.* **81**, 3464 (2002).
- <sup>15</sup>E. Joselevich and C. M. Lieber, *Nano Lett.* **2**, 1137 (2002).
- <sup>16</sup>K. P. Cheung and C. P. Chang, *J. Appl. Phys.* **75**, 4415 (1994).
- <sup>17</sup>S. Fang and J. P. McVittie, *J. Appl. Phys.* **72**, 4865 (1992).
- <sup>18</sup>S. Ma, J. P. McVittie, and K. C. Saraswat, *IEEE Electron Device Lett.* **18**, 468 (1997).
- <sup>19</sup>B. Chapman, *Glow Discharge Processes* (Wiley, New York, 1980), Vol. 1, p. 56.
- <sup>20</sup>See EPAPS Document No. E-APPLAB-91-033751 for supporting information. This document can be reached through a direct link in the online article's HTML reference section or via the EPAPS homepage (<http://www.aip.org/pubservs/epaps.html>).
- <sup>21</sup>W. Merchan-Merchan, A. V. Saveliev, and L. A. Kennedy, *Carbon* **42**, 599 (2004).
- <sup>22</sup>F. Xu, X. Liu, and S. D. Tse, *Carbon* **44**, 570 (2006).
- <sup>23</sup>C. Bower, W. Zhu, S. Jin, and O. Zhou, *Appl. Phys. Lett.* **77**, 830 (2000).
- <sup>24</sup>J. Li, Q. Ye, A. Cassell, H. T. Ng, R. Stevens, J. Han, and M. Meyyappan, *Appl. Phys. Lett.* **82**, 2491 (2003).
- <sup>25</sup>H. Y. Yap, B. Ramaker, A. V. Sumant, and R. W. Carpick, *Diamond Relat. Mater.* **15**, 1622 (2006).